Title Page

Names of authors: Sho Ogasawara[1, 5], Atsushi Nakao[1], Tetsuya Eguchi[2], Takeshi Ota[3], Hisaya Matsunami[2], Junta Yanai[1], Takuro Shinano[4]

Title: Extractability of potassium and radiocaesium in soils developed from granite and sedimentary rock in Fukushima, Japan

Affiliations and addresses of the authors:

[1] Graduate School of Life and Environmental Sciences, Kyoto Prefectural University, Kyoto 606-8522, Japan

[2] Tohoku Agricultural Research Centre, NARO, Fukushima 960-2156, Japan

[3] Bio-oriented Technology Research Advancement Institution, NARO, 210-0005 Kanagawa, Japan

[4] Graduate School of Agriculture, Hokkaido University, Hokkaido 060-8589, Japan

[e] Japan Society for the Promotion of Science, 102-0083 Tokyo, Japan

E-mail address of the corresponding author:

Sho Ogasawara (shooga.0206@gmail.com)

The extractability of potassium and radiocaesium in soils developed from granite and sedimentary rock in Fukushima, Japan

Sho Ogasawara[1, 5], Atsushi Nakao[1], Tetsuya Eguchi[2], Takeshi Ota[3], Hisaya Matsunami[2], Junta Yanai[1], Takuro Shinano[4]

[1] *Graduate School of Life and Environmental Sciences, Kyoto Prefectural University, 606-8522 Kyoto, Japan*

[2] *Tohoku Agricultural Research Centre, NARO, 960-2156 Fukushima, Japan*

[3] *Bio-oriented Technology Research Advancement Institution, NARO, 210-0005 Kanagawa, Japan*

[4] *Graduate School of Agriculture, Hokkaido University, 060-8589 Hokkaido, Japan*

[5] *Japan Society for the Promotion of Science, 102-0083 Tokyo, Japan*

Abstract

Potassium (K) and radiocaesium (RCs) were chemically extracted from soils derived from granite (G soils) and sedimentary rock (S soils) in Fukushima, Japan. The

extractants employed were 1 M HNO_3, concentrated HNO_3, and HF + $HClO_4$. As S soils contain a lower amount of trioctahedral 2:1 phyllosilicates than G soils, the RCs/K ratio was higher in S soils than in G soils with 1 M HNO_3 extraction, indicating that the potential risk of soil-to-plant transfer of RCs is higher in S soils than in G soils. In conclusion, information about surface geology is important in predicting the spatial pattern of soil characteristics related to transferability of RCs.

Keywords

agricultural soils, Fukushima prefecture, micaceous mineral, potassium, radiocaesium

Introduction

Phytoavailability of potassium (K) in soil is one of the most important factors in controlling the transfer of radiocaesium (RCs) from soil to plants. For the similar effective ionic radii of K and RCs, K competes with RCs at the ionic transporter in the root system [1, 2]. Therefore, uptake of RCs by plants is restricted in soils with a higher content of phytoavailable K, which is generally distinguished between exchangeable K [3–5] and nonexchangeable K [6, 7]. The exchangeable K is bound to soil components with weak

electrostatic power and can be thus absorbed readily by plants. In Fukushima prefecture, an exchangeable K content of >210 mg K kg soil^{-1} is recommended to reduce transfer of RCs from the soil to plants based on the findings by Kato et al. [4]. Nonexchangeable K is retained more strongly in the soil and released more slowly than exchangeable K. Therefore, it is a secondary important reservoir of phytoavailable K, which can be utilized by plants once exchangeable K has been exhausted in the soil adjacent to the root surface (i.e., rhizosphere). Although little attention has been devoted to the effect of nonexchangeable K on the phytoavailability of RCs, recent research has shown that it is important in soils that have a low content of exchangeable K [7].

Nonexchangeable K is retained mainly in the interlayer of micaceous minerals (micas). As the interlayer site in mica can also adsorb RCs strongly, mica is considered to be a reservoir of both RCs and nonexchangeable K. Mica can be categorized into two types, i.e., trioctahedral mica (e.g., biotite) and dioctahedral mica (e.g., illite), based on the number of metal cations occupying the octahedral structure. Trioctahedral mica is known to be able to release its interlayer K^+ more readily than the dioctahedral mica [8]. Which of the two types is dominant in a particular soil is highly relevant to surface geology. In the eastern Fukushima prefecture, surface geology can be divided into granite and

64 sedimentary rock [9]. Biotite is dominant in soils derived from granite (G soils) [10],
65 whereas illite is dominant in soils derived from sedimentary rock (S soils) [11]. Given the
66 relevance of geology to soil mineralogy, it is very likely that G soils have a higher
67 nonexchangeable K content than S soils and, therefore, a lower risk of soil-to-plant
68 transfer of RCs. Few studies in Fukushima prefecture evaluated the difference in the
69 nonexchangeable K content of soils with different geological backgrounds. Therefore,
70 this study aims to investigate the relative abundance of di- or trioctahedral minerals in
71 soils in Fukushima prefecture and clarify the relationship between the mineralogy and
72 extractability of K and RCs from soils with different geological backgrounds.

73 **Materials**

74 Twenty-eight soil samples were collected at depths of 0–10 cm from 14 agricultural
75 fields in granitic areas (sample names: G1–G14) and 14 fields in sedimentary rock
76 areas (S1–S14) in Fukushima prefecture. The G12 and G13 soils were sampled from
77 a buckwheat field and from pasture, respectively. The remaining soil samples were
78 collected from paddy fields, including fallow fields. Surface geology was assessed
79 on the basis of the surface geology map produced by AIST [9]. The sampling
80 locations and the geology map are shown in Fig. 1. This sample set did not include

81 decontaminated soils because the decontamination procedure generally involves
82 applying uncontaminated soil brought from other areas [12]. The soil samples were
83 air-dried and sieved using ≤2-mm mesh. During sieving, as many plant residues as
84 possible were removed using tweezers.

85 **Experimental**

86 **1. Mineralogical analysis**

87 The types of phyllosilicate minerals, di- and/or trioctahedral, contained in the soil
88 were distinguished by (060) reflections of powdered X-ray diffraction (XRD)
89 analysis (SmartLab-FE, Rigaku, Tokyo, Japan, CuKα radiation). A 3-g portion of
90 soil was suspended in water via ultrasonic treatment, and wet sieving and freeze-
91 drying were used to collect the clay–silt fraction (particle diameter ≤20 μm) in the
92 soil. The dried particles were ground softly using a ceramic pestle and mortar.
93 Removal of organic matter and iron oxides, which are standard pretreatments for
94 XRD analysis of soils' clays, was avoided because these treatments alter the structure
95 of iron-bearing 2:1 clay minerals via either oxidative or reductive reactions [13]. A
96 portion of the powdered clay–silt fraction was oriented randomly on a glass slide and
97 scanned from 59° to 63° 2θ, with steps of 0.0050° 2θ and a scan speed of 0.1° 2θ

98 min^{-1}. Areas of the diffraction peaks recorded were quantified by decomposition into
99 a Lorentzian-shaped peak using PeakFit software ver. 4.12 (SeaSolve Software Inc.,
100 Framingham, MA).

101 **2. Chemical extractions**

102 Potassium and RCs were extracted from soils using three methods: hot 1 M nitric
103 acid (HNO_3) extraction (Ex. 1), concentrated HNO_3 extraction (Ex. 2), and residue
104 decomposition (Ex. 3). The Ex. 1 was almost the same as the extraction procedure
105 for phytoavailable K in soil [14]. The Ex. 2 was the modified method of the "strong
106 acid dissolution" by Saito et al. [15]. The Ex. 3 was the decomposition of the residue
107 that remained after the Ex. 2 using hydrofluoric acid (HF) and perchloric acid
108 ($HClO_4$).

109 Ex. 1 (hot 1 M HNO_3 extraction): A 10-g portion of soil and 100 mL of 1 M HNO_3
110 were mixed in a 200-mL Erlenmeyer flask and preheated on a hotplate for 20 min
111 until boiling and then heated for a further 15 min. After heating, the flask was allowed
112 to cool for 5 min at room temperature, and the suspension was filtered using filter
113 paper. The residue on the filter paper was washed using 0.1 M HNO_3. The filtrate

was then filtered using a 0.45-µm syringe filter and brought up to 100 mL with 0.1 M HNO_3.

Ex. 2 (concentrated HNO_3 extraction): A 5-g portion of soil and 25 mL 13.4 M HNO_3 (density = 1.38) were mixed in a Teflon beaker and heated on a hotplate for 3 h at 100°C. After heating, the suspension was diluted with ultrapure water, centrifuged to recover the residue, and filtered using a 0.45-µm syringe filter. The filtrate was brought up to 100 mL with pure water. The residue was dried in an oven overnight at 105°C.

Ex. 3 (digestion of residue): The dried residue was powdered using a tungsten carbide pestle and mortar. A 0.5-g portion of powdered soil was weighed into a Teflon beaker and digested using HF and $HClO_4$ while being heated on a hotplate. The decomposed products were dissolved using hydrogen chloride and HNO_3 and brought up to 50 mL.

The above extractions were performed in duplicate. The Ex. 1 and Ex. 2 were performed independently, and not subsequently, to obtain higher concentrations of RCs in the extracted solution for more precise radiometric analyses. The amount of K and RCs extracted using Ex. 1 was denoted as fraction 1 (F1). The fraction 2 (F2)

was calculated by subtracting the amounts of K or RCs in the Ex.1 solutions from those in the Ex. 2 solutions. The amount of K and RCs extracted using Ex. 3 was denoted as fraction 3 (F3).

3. Quantification of K and RCs

The K concentrations in the Ex. 1, Ex. 2, and Ex. 3 solutions were determined using atomic absorption spectrometry (ZA-3000, Hitachi High-Technologies Corporation, Tokyo, Japan). The RCs dissolving in the Ex. 1 and Ex. 2 solutions were concentrated via the ammonium phosphomolybdate (AMP) method [16] and determined using a sodium iodide (NaI) scintillation counter (2480 WIZARD^2, Perkin Elmer, MA, USA), with a relative standard deviation (RSD) of <5 %. The AMP has a strong ability to adsorb Cs^+ and has low solubility in water and particularly in nitric acid [17]; therefore, RCs in the acidic solution can be concentrated and recovered as an AMP-Cs compound. As described in detail by Aoyama and Hirose [16], approximately 0.2 g of AMP was added to the Ex. 1 and Ex. 2 solutions and stirred with a magnetic stirrer for 1 h, and the AMP-Cs compound was recovered on the next day using the 0.45-μm filter. The collected AMP-Cs compound was dissolved using 2 mL of 1 M sodium hydroxide in a 75-mm-long polypropylene tube with a

12-mm radius for geometry matching, and the RCs content was measured using an NaI scintillation counter (2480 WIZARD^2, Perkin Elmer, MA, USA), with an RSD of <5 %. The RCs concentrations in the Ex. 3 solutions were not determined directly, but the RCs concentration in F3 was calculated by subtracting those in F1 and F2 from the total RCs concentration in the soil. The total RCs concentration in soil was calculated from the total concentration of ^{137}Cs in soil and the half-life of ^{137}Cs (30.1 y) and ^{134}Cs (2.07 y) assuming that RCs is the sum of ^{137}Cs and ^{134}Cs and that the ^{137}Cs/^{134}Cs activity ratio was 1.0 at the time of the Fukushima Dai-ichi Nuclear Power Plant accident [18]. The total ^{137}Cs concentration in soil was determined using the Ge semiconductor detector (GC2520, Canberra, Meriden, CT, USA), with an RSD of <5%.

Results and Discussions

1. Mineralogy of soil samples

The XRD patterns at 59–63 °2θ of the clay–silt fraction from G and S soils are shown in Fig. 2. All the samples exhibited four prominent peaks at approximately 59.9 °2θ, 60.1 °2θ, 61.8 °2θ, and 62.3 °2θ, corresponding to the presence of quartz (Qz), trioctahedral mineral (Tri), dioctahedral mineral (Di), and kaolinite (Kl), respectively

[19]. The peak positions for Tri and Qz and those for Di and Kl were close enough to overlap with each other. The G soils exhibited prominent Tri peaks, but they exhibited a very small Di peak that was nearly concealed by the adjacent large Kl peaks, suggesting that these soils were enriched with trioctahedral phyllosilicates. In contrast, most of the S soils exhibited a prominent Di peak together with a distinct Tri peak, suggesting that these soils contained both di- and trioctahedral phyllosilicates. Trioctahedral phyllosilicates in the S soils may have been transported there by streams running through granite in the uplands.

Table 1 shows the peak areas of Tri and Di. The peak areas in the powder XRD may vary depending on the amount of sample oriented on glass slides. Hence, we determined the ratios of Tri peak areas against the sum of the Tri and Di peak areas (Tri/Di+Tri) as a quantitative indicator of the relative abundance of trioctahedral phyllosilicates. For G soils, the average value of Tri/Di+Tri was 0.72, whereas it was 0.43 for S soils. The Tri/Di+Tri values for G soils were significantly higher ($P <$ 0.01) than those for S soils, which is a direct indication that the G soils contained a higher amount of trioctahedral minerals than the S soils. Relatively low Tri/Di+Tri

181 values for G5, G11, and G12 also corresponded with the presence of Di peaks in their
182 XRD patterns (Fig. 2).

183 **2. The extractability of RCs and K**

184 Individual data on the extractability of K and RCs from soils are presented in Table
185 2, and their summary data are shown as boxplots in Fig. 3 and Fig. 4, respectively.
186 For G soils, the medians of K extractability were 5.0% in F1, 13.3% in F2, and 82.5%
187 in F3, whereas those for S soils were 2.7% in F1, 2.6% in F2, and 94.9% in F3. In G
188 soils, the K extractability in F1 and F2 was significantly higher than that in S soils,
189 confirming that the phytoavailable K content in G soils is higher than that in S soils.
190 However, even in G soils, the K extractability of G soils with Di peaks (G5, G11,
191 and G12) was relatively low. The K extractability for G5, G11, and G12 in F1 were
192 1.4%, 2.3%, and 3.0 %, respectively, and the corresponding values in F2 were 2.9%,
193 6.3%, and 7.7%, respectively (Table 2). These values were lower than the medians
194 of K extractability for G soils, indicating lower contribution of dioctahedral mica to
195 the K supply.

196 For G soils, the medians of extractability of RCs were 20.4% in F1, 16.8% in F2, and
197 61.7% in F3, whereas those for S soils were 25.6% in F1, 28.6% in F2, and 44.6% in

198 F3. In contrast to those of K, the medians of extractability of RCs in F1 and F2 for
199 G soils were lower than those for S soils and the extractability of RCs in F3 for G
200 soils was significantly higher than that for S soils. This higher persistence in F3 for
201 G soils may be linked to these soils having a larger amount of fixation sites for RCs
202 than is the case with S soils. Fixation of RCs in soil occurs on the weathered edge of
203 mica, known as the frayed edge site (FES) [20]; Ogasawara et al. [7] showed that S
204 soils had lower FES content than G soils. A higher FES content in soil is responsible
205 for the lower extractability of RCs by ammonium ions (NH_4^+) [7, 21, 22] and by 0.1
206 M hydrochloric acid [22] while these methods extract RCs adsorbed on soil more
207 weakly than extractions performed in this study. The effect of the FES content in soil
208 on the strength of the adsorption of RCs should be examined further.

209 **3. RCs uptake risk assessment based on the extractability of RCs and K**

210 Kondo et al. [23] reported that the relative extractability of ^{137}Cs to K by NH_4^+ was
211 proportional to the concentration of ^{137}Cs in plants, indicating that higher
212 extractability of RCs and/or lower extractability of K results in a higher uptake of
213 RCs by plants. In addition, in the current study, we calculated the relative
214 extractability of RCs to K (RCs/K) was calculated to assess the risk of uptake of RCs

by plants (Table 3). These summary data are presented as a boxplot in Fig. 5. The median values of RCs/K for G soils were 3.7 in F1, 1.3 in F2, and 0.8 in F3, whereas the values for S soils were 9.6 in F1, 12.5 in F2, and 0.5 in F3. The RCs/K value for G soils was significantly lower than that for S soils in F1 (P <0.05) and F2 (P < 0.001), and the RCs/K value in F3 for G soils was significantly higher (P < 0.01) than that for S soils, indicating that G soils have a lower risk of transfer of RCs than S soils. This finding corresponds with those of previous studies reported that uptake of RCs by rice in granite areas was smaller than that in sedimentary rock areas [7, 24]. Moreover, RCs/K values in F1 were negatively correlated (P < 0.001) with Tri/Di+Tri values (Fig. 6). This relationship indicated that soils containing more trioctahedral minerals have lower risk of RCs uptake by plants. Although most of the G soils were plotted in the lower-right area, G soils with a Di peak, especially G5 and G 11, were plotted in the upper-left area. This indicated that some G soils have lower trioctahedral mineral contents and, hence, have a higher risk of uptake of RCs by plants. Therefore, use of XRD analysis data as supporting information for surface geology would be an effective and more reliable method to estimate the relative risk of transfer of RCs from soils to plants.

Conclusion

The effect of mica type, either trioctahedral mica or dioctahedral mica, in soil on the extractability of K and RCs was examined using G soils and S soils. The release of more K and less RCs from G soils than from S soils demonstrated that the risk of uptake of RCs by plants is potentially lower in G soils than in S soils. Though surface geology is useful in estimating whether either trioctahedral mica or dioctahedral mica is dominant in the soil, some soils in granite areas can have relatively lower contents of trioctahedral minerals. The combined use of surface geology information and XRD analysis would be a more effective and reliable approach for estimating the risk of transfer of RCs from soils to plants.

Acknowledgments

Gratitude is expressed to the Food Safety and Consumer Affairs Bureau, MAFF, prof. Shin Moono (Faculty of Food and Agricultural Sciences, Fukushima University), Dr. Yuzo Manpuku (Institute for Agro-Environmental Sciences, NARO), Dr. Tomoaki Nemoto (Fukushima Prefectural Government), Dr. Takashi Saito (same as above), Mr. Kazuhiro Kohata (same as above), and the agricultural department of Minamisoma city and Namie town who helped soil samples collection. Authors also appreciate Ms. Yuko

Abe (Tohoku Agricultural Research Centre, NARO) for the help of experiments. The authors would like to thank Enago (www.enago.jp) for the English language review. Analyses of RCs measurements were carried out in the Laboratory of Radioisotopes of Kyoto Prefectural University.

Funding

This work was financially supported by the JSPS KAKENHI [grant number JP15J06569 and 16H06188].

References

1. Smolders E, Van Den Brande K, Merckx R (1997) Concentrations of ^{137}Cs and K in soil solution plant availability of ^{137}Cs in soils. Environ Sci Technol. 31, 12: 3432–3438

2. White PJ, Broadley MR (2000) Mechanisms of caesium uptake by plants.New Phytol. 147, 2: 241–256

3. MAFF (2014) Causes of contamination by radiocesium and countermeasures for these problems.Minist Agric For Fish. 0–24

4. Kato N, Kihou N, Fujimura S, Ikeba M, Miyazaki N, Saito Y, Eguchi T, Itoh S (2015) Potassium fertilizer and other materials as countermeasures to reduce radiocesium levels in rice: Results of urgent experiments in 2011 responding to the Fukushima Daiichi Nuclear Power Plant accident. Soil Sci Plant Nutr. 61: 179–190

5. Kubo K, Fujimura S, Kobayashi H, Ota T, Shinano T (2017) Effect of soil exchangeable potassium content on cesium absorption and partitioning in buckwheat grown in a radioactive cesium-contaminated field. Plant Prod Sci. 2017.

6. Eguchi T, Ohta T, Ishikawa T, Matsunami H, Takahashi Y, Kubo K, Yamaguchi N, Kihou N, Shinano T (2015) Influence of the nonexchangeable potassium of mica on radiocesium uptake by paddy rice.J Environ Radioact.147: 33–42

7. Ogasawara S, Eguchi T, Nakao A, Fujimura S, Takahashi Y, Matsunami H, Tsukada H, Yanai J, Shinano T (2019) Phytoavailability of ^{137}Cs and stable Cs in soils from different parent materials in Fukushima, Japan. J Environ Radioact. 198: 117–125

8. Fanning D, Keramidas V, El-Deskoy M (1989) Micas. In: Dixon JB, Weed SB (Eds.), Minerals in Soil Environments, Soil Sci Soc Am, Madison, 551–634

9. AIST (ed.), Geological Survey of Japan 2014. Seamless digital geological map of Japan 1: 200,000. Jan 14, 2014 version, Geological Survey of Japan, National Institute of Advanced Industrial Science and Technology

10. Mukai H, Hatta T, Kitazawa H, Yamada H, Yaita T, Kogure T (2014) Speciation of radioactive soil particles in the Fukushima contaminated area by IP autoradiography and microanalyses. Environ Sci Technol. 48, 22: 13053–13059

11. Ramseyer K, Boles JR (1986) Mixed-layer illite/smectite minerals in tertiary sandstones and shales, San Joaquin Basin, California. Clays Clay Miner. 34, 2: 115–124

12. Fukushima Prefectural Government, 2018 http://www.pref.fukushima.lg.jp/site/portal-english/en02-03.html (accessed on Aug. 20, 2019)

13. Ross GJ, Rich CI (1974) Effect of oxidation and reduction on potassium exchange of biotite. Clays Clay Miner. 22, 4: 355–360

296 14. Helmke PA, Sparks DL (1996) Lithium, Sodium, Potassium, Rubidium, and Cesium.
297 In: Sparks, D. L. (Ed.), Methods of soil analysis Part 3–Chemical methods, SSSA
298 Book Series. no. 5, Madison, WI, 560–563.

299 15. Saito T, Makino H, Tanaka S (2014) Geochemical and grain-size distribution of
300 radioactive and stable cesium in Fukushima soils: Implications for their long-
301 term behavior. J Environ Radioact. 138: 11–18

302 16. Aoyama M, Hirose K (2008) Radiometric determination of anthropogenic
303 radionuclides in seawater. Radioact Environ. 11: 137–162

304 17. Budavari S, O'Neil MJ, Smith A, Heckelman PE, Kinneary JF (Eds) (1996) The
305 Merck Index, An Encyclopedia of Chemicals, Drugs, and Biologicals (12th
306 ed.). Merck & Co., Inc., New Jersey, 589

307 18. Hirose K (2012) 2011 Fukushima Dai-ichi nuclear power plant accident: Summary
308 of regional radioactive deposition monitoring results. J Environ Radioact. 111:
309 13–17

310 19. Moore DM, Reynolds RC Jr. (1997) Identification of clay minerals and associated
311 minerals, In: X-ray diffraction and the identification and analysis of clay minerals
312 (Second Edition). Oxford University Press, Madison, NY, 227–260.

20. Sawhney BL (1972) Selective sorption and fixation of cations by clay minerals: A review. Clays Clay Miner. 20: 93–100

21. Delvaux B, Kruyts N, Cremers A (2000) Rhizospheric mobilization of radiocesium in soils. Environ Sci Technol. 34, 8: 1489–1493

22. Vandebroek L, Hees MV, Delvaux B, Spaargaren O, Thiry Y (2012) Relevance of radiocaesium interception potential (RIP) on a worldwide scale to assess soil vulnerability to ^{137}Cs contamination. J Environ Radioact. 104: 87–93

23. Kondo M, Maeda H, Goto A, Nakano H, Kiho N, Makino T, Sato M, Fujimura S, Eguchi T, Hachinohe M, Hamamatsu S, Ihara H, Takai T, Arai-Sanoh Y, Kimura T (2015) Exchangeable Cs/K ratio in soil is an index to estimate accumulation of radioactive and stable Cs in rice plant. Soil Sci Plant Nutr. 61: 133–143

24. Yamamura K, Fujimura S, Ota T, Ishikawa T, Saito T, Arai Y, Shinano T (2018) A statistical model for estimating the radiocesium transfer factor from soil to brown rice using the soil exchangeable potassium content. J Environ Radioact. 195: 114–125

329 **Table 1** Peak areas of tri- (Tri) and dioctahedral minerals (Di) contained in (a) G
330 soils and (b) S soils and the peak area ratio of trioctahedral minerals against the sum
331 of di- and trioctahedral minerals.

(a)

Sample name	Peak area		Tri/Di+Tri
	Tri	Di	
G1	1490	1120	0.57
G2	1910	809	0.70
G3	3050	583	0.84
G4	1910	267	0.88
G5	1030	1620	0.39
G6	2940	681	0.81
G7	1620	380	0.81
G8	1170	473	0.71
G9	2470	729	0.77
G10	1350	597	0.69
G11	1080	1380	0.44
G12	1230	1040	0.54
G13	1850	42.8	0.98
G14	1630	158	0.91
average	1770	706	0.72

(b)

Sample name	Peak area		Tri/Di+Tri
	Tri	Di	
S1	930	2410	0.28
S2	776	2160	0.26
S3	596	2190	0.21
S4	647	2310	0.22
S5	1270	1590	0.44
S6	2340	1110	0.68
S7	1800	494	0.78
S8	715	261	0.73
S9	2330	1590	0.59
S10	1130	5540	0.17
S11	2020	1760	0.53
S12	1920	1580	0.55
S13	1770	5240	0.25
S14	872	2100	0.29
average	1370	2170	0.43

332

333

334 **Table 2** Extractability of K and RCs for G soils and S soils

	sample name	K extractability							RCs extractability						
		F1		F2		F3		Total	F1		F2		F3		Total
		(g kg^{-1})	(%)	(g kg^{-1})	(%)	(g kg^{-1})	(%)	(g kg^{-1})	(Bq kg^{-1})	(%)	(Bq kg^{-1})	(%)	(Bq kg^{-1})	(%)	(Bq kg^{-1})
G soils	G1	0.71	6.6	0.64	6.0	9.4	87	10.8	220	23	130	14	610	64	960
	G2	1.14	5.2	2.10	10	18.6	85	21.9	370	34	120	11	610	55	1100
	G3	0.63	3.1	2.20	11	17.9	86	20.8	330	24	380	27	690	49	1400
	G4	0.98	5.3	2.79	15	14.8	80	18.6	450	26	490	29	760	45	1700
	G5	0.37	1.4	0.78	2.9	25.6	96	26.7	1700	31	900	17	2800	52	5400
	G6	1.69	12	3.63	25	9.2	63	14.5	260	20	170	13	870	67	1300
	G7	0.76	5.6	3.00	22	9.8	72	13.6	320	17	370	19	1200	63	1900
	G8	0.80	4.8	2.95	18	12.8	77	16.5	190	11	450	26	1100	65	1700
	G9	1.43	8.4	5.08	30	10.5	62	17.1	220	17	190	15	890	68	1300
	G10	0.80	4.7	3.58	21	12.8	74	17.2	220	18	160	13	820	68	1200
	G11	0.55	2.3	1.52	6.3	22.0	91	24.1	220	22	170	17	610	61	1000
	G12	0.75	3.0	1.92	7.7	22.4	89	25.0	140	10	110	8	1200	86	1400
	G13	2.01	13	4.85	32	8.3	55	15.1	430	18	550	23	1400	58	2400
	G14	0.93	3.0	3.57	12	26.1	85	30.6	29000	21	55000	39	56000	40	140000
S soils	S1	0.43	2.6	0.19	1.2	15.6	96	16.3	990	29	810	24	1600	47	3400
	S2	0.55	3.9	0.48	3.4	12.9	93	13.9	2300	29	2400	31	3100	40	7800
	S3	0.32	2.7	0.31	2.6	11.1	95	11.7	1100	30	1200	32	1400	38	3700
	S4	0.46	3.9	0.37	3.1	11.0	93	11.8	520	20	780	30	1300	50	2600
	S5	0.74	4.4	1.05	6.2	15.0	89	16.8	11000	25	12000	27	21000	48	44000
	S6	0.24	1.1	0.13	0.6	21.3	98	21.6	150	10	370	25	980	65	1500
	S7	0.42	2.6	0.35	2.2	15.3	95	16.1	150	8	520	27	1200	63	1900
	S8	0.53	2.8	0.15	0.8	18.2	96	18.8	230	15	230	15	1000	67	1500
	S9	0.88	5.5	1.13	7.1	14.0	87	16.0	380	25	370	25	750	50	1500
	S10	0.26	1.1	0.37	1.6	22.4	97	23.0	310	26	400	33	490	41	1200
	S11	0.53	2.8	0.91	4.8	17.3	92	18.8	410	29	460	33	530	38	1400
	S12	0.53	2.8	1.28	6.7	17.4	91	19.2	530	33	470	29	600	38	1600
	S13	0.33	1.4	0.60	2.5	22.5	96	23.4	270	23	490	41	440	37	1200
	S14	0.40	2.0	0.44	2.2	19.2	96	20.0	570	30	530	28	800	42	1900

335

336

337 **Table 3** Relative extractability of RCs to K

	sample name	RCs/K		
		F1	F2	F3
G soils	G1	3.4	2.3	0.73
	G2	6.4	1.1	0.65
	G3	7.7	2.6	0.57
	G4	5.0	1.9	0.56
	G5	23	5.7	0.54
	G6	1.7	0.5	1.06
	G7	3.0	0.9	0.87
	G8	2.3	1.5	0.84
	G9	2.0	0.5	1.1
	G10	3.9	0.6	0.92
	G11	9.6	2.7	0.67
	G12	3.3	1.0	0.96
	G13	1.4	0.7	1.1
	G14	6.8	3.4	0.47
S soils	S1	11	20	0.49
	S2	7.5	9.0	0.43
	S3	11	12	0.40
	S4	5.2	9.6	0.54
	S5	5.7	4.4	0.53
	S6	8.9	41	0.66
	S7	3.0	13	0.66
	S8	5.5	19	0.69
	S9	4.6	3.5	0.57
	S10	23	21	0.42
	S11	10	6.8	0.41
	S12	12	4.4	0.41
	S13	16	16	0.38
	S14	15	13	0.44

338

339

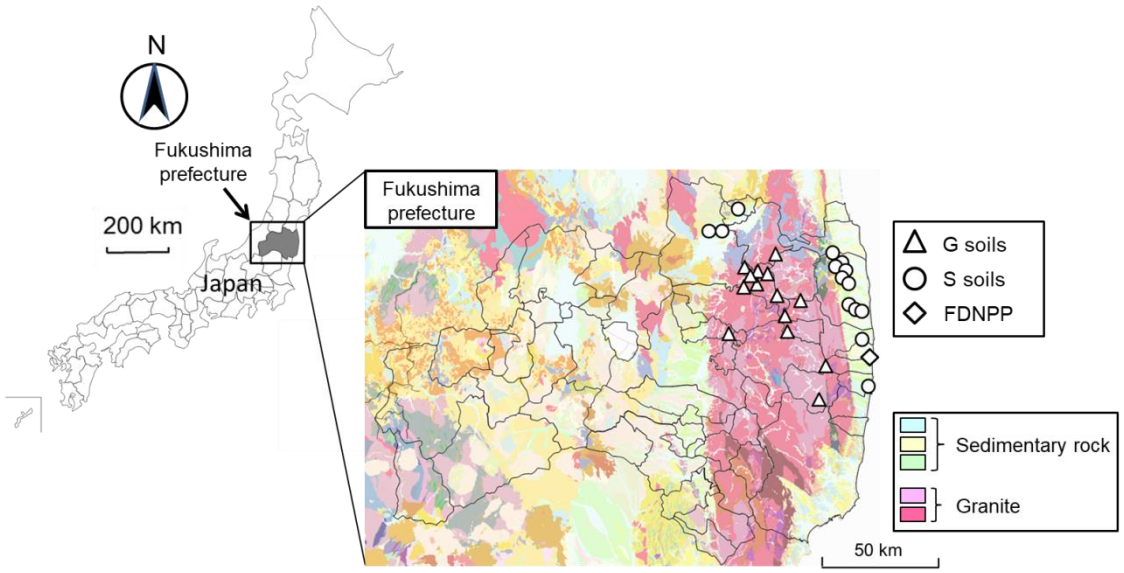

340

341 **Fig. 1** Locations of the soils collected and their surface geology. The geological map
342 was adopted from 1:20,000Seamless Digital Geological Map of Japan in Geomap
343 Navi (https://gbank.gsj.jp/geonavi/geonavi.php) by Geological Survey of Japan,
344 AIST (2014). Authors combined it with blank map downloaded from
345 (https://n.freemap.jp/). The other information including scales, direction, and legends
346 were added by authors. Detailed legends are available online
347 (https://gbank.gsj.jp/seamless/legend_e.html).

348

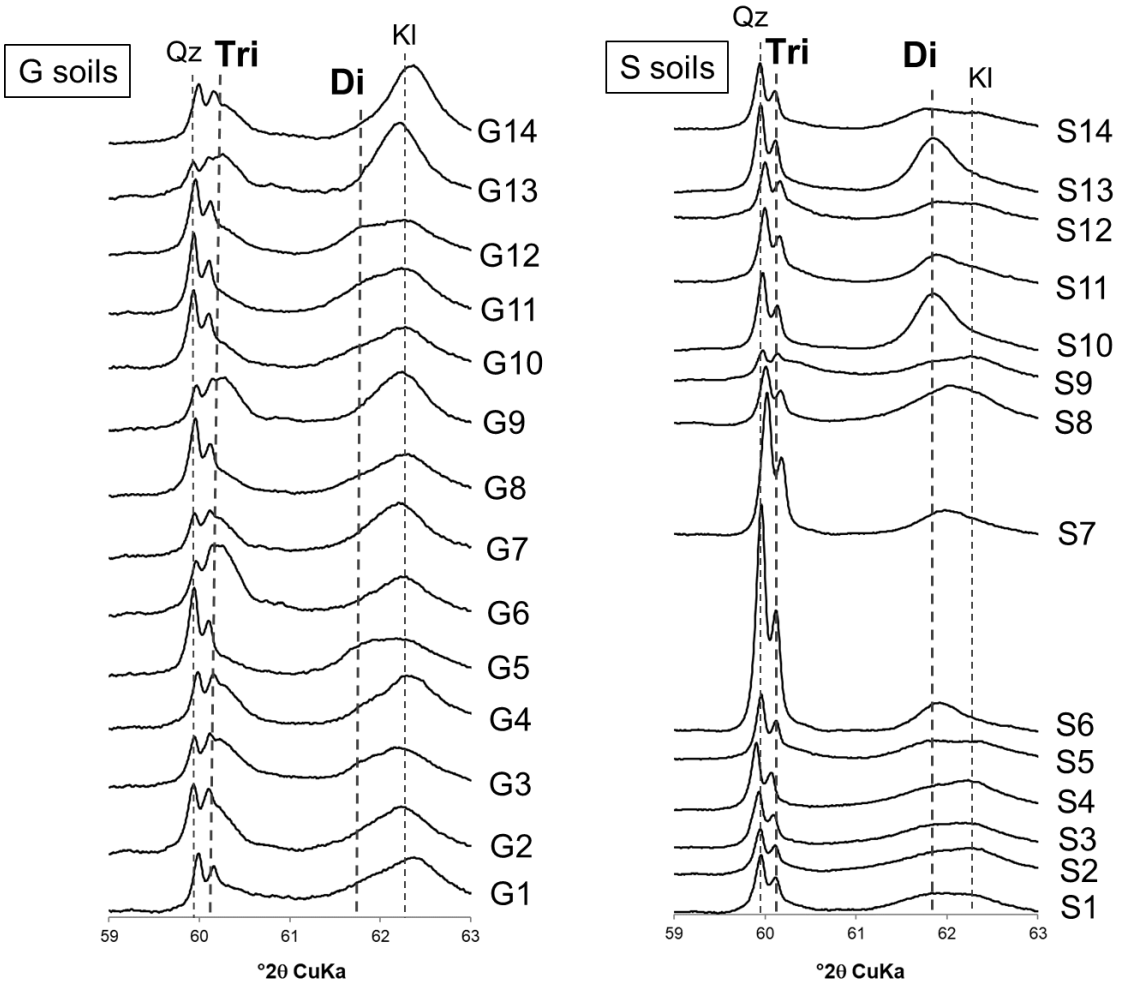

Fig. 2 X-ray diffraction patterns for clay-silt fraction collected from soil samples.

Abbreviations; Qz: Quartz, Tri: Trioctahedral mineral, Di: Dioctahedral mineral, Kl: Kaolinite

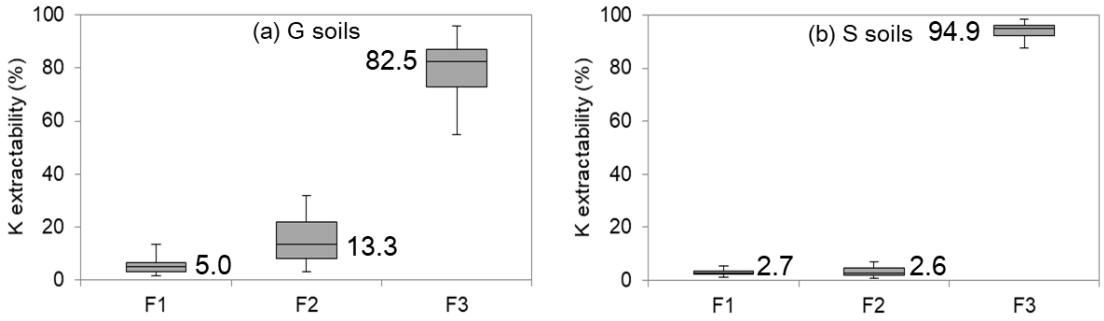

354

355 **Fig. 3** The extractability of K for (a) G soils and (b) S soils in each fraction. The grey

356 colored boxes describe the range of 25–75th percentiles and the horizontal line means

357 the median value. The vertical lines describe the range of maximum and minimum

358 values.

359

360

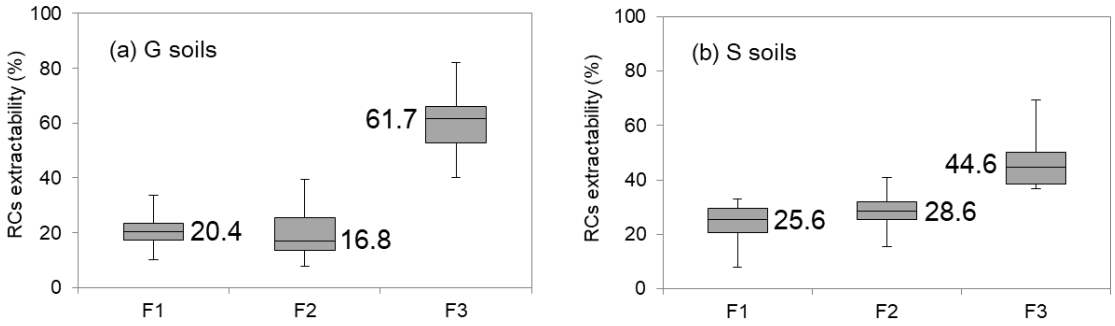

Fig. 4 The extractability of RCs for (a) G soils and (b) S soils in each fraction. The grey colored boxes describe the range of 25–75th percentiles and the horizontal line means the median value. The vertical lines describe the range of maximum and minimum values.

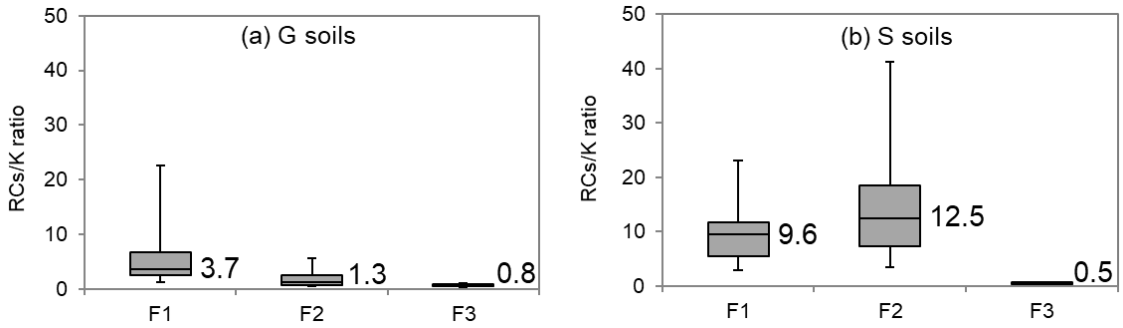

366

367 **Fig. 5** The ratios of the RCs extractability against that of K for (a) G soils and (b) S

368 soils in each fraction. The grey colored boxes describe the range of 25–75th

369 percentiles and the horizontal line means the median value. The vertical lines

370 describe the range of maximum and minimum values.

371

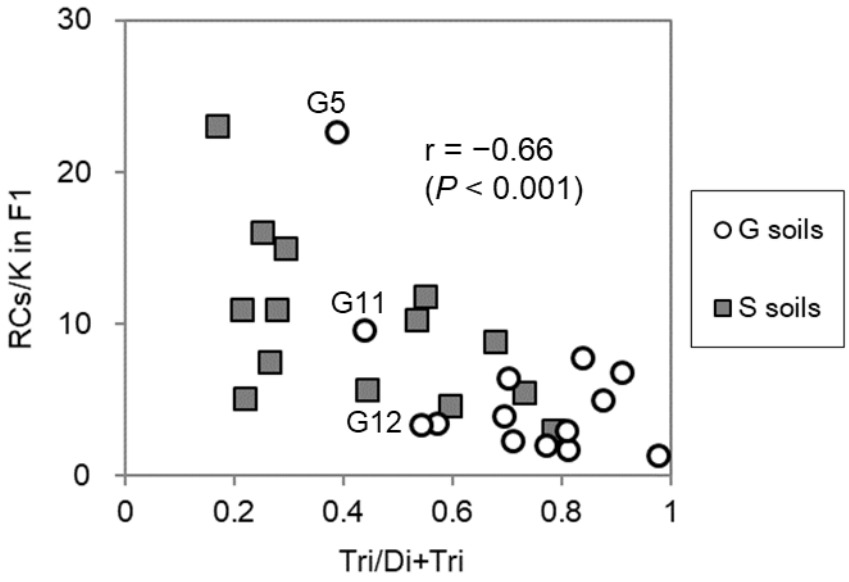

372

373 **Fig. 6** The relationship between the Tri/Di+Tri and the extractability of RCs against

374 K in F1. (r: Pearson's correlation coefficient)

375